Monomer-Capped Tin Metal Nanoparticles for Anode Materials in Lithium Secondary Batteries

Mijung Noh,[†] Yoojin Kim,[†,‡] Min Gyu Kim,[‡] Hyojin Lee,[†] Hyunjung Kim,[†] Yoojung Kwon,[†] Youngil Lee,[§] and Jaephil Cho*[,†]

Department of Applied Chemistry, Kumoh National Institute of Technology, Gumi, Korea, Beamline Research Division, Pohang Accelerator Laboratory, Pohang University of Science and Technology, Pohang, Korea, and Department of Chemistry, University of Ulsan, Ulsan, Korea

Received February 25, 2005
Revised Manuscript Received May 20, 2005

The synthesis and characterization of metal nanoparticles have attracted a great deal of attention due to their potential applications in magnetics, electronics, and catalysis.[1] The properties of the protective ligands greatly influence the particle size and the dispersity of metal nanoparticles.[2,3] In this regard, Fe, Pd, Co, Pt, or their alloys have been intensively investigated.[4−7] On the other hand, Sn metal has not received much attention, and Bönnemann et al. first studied microcrystalline tin particles reduced from $SnCl_2$ using $LiBEt_3H$ in THF at room temperature but the particle size was not reported.[8] Nayral et al. reported the synthesis of Sn/SnO_2 nanoparticles prepared by decomposition of tin(II) amides ($Sn(NMe_2)_2)_2$) at 135 °C in dry anisole, and the particle size was <100 nm.[9] However, no evidence for Sn metal phase formation was provided, and oxygen content was estimated to 8 wt % from energy dispersive X-ray analysis (EDXA). In contrast, Schlecht et al. tried to vary the particle size of the nanocrystalline tin by changing the $SnCl_4$ concentration in THF before reduction with $Li[Et_3BH]$.[10] However, the concentration of the solution of $SnCl_4$ had no effect on the particle size, and tin particles of 40−50 nm size were obtained. Soulantica et al. reported that UV radiation (365 nm) of $\{Sn(NMe_2)_2]_2\}$ in toluene at room temperature in the absence of stirring and in the presence of 1 equiv of hexadecylaime led to the formation of ∼50 nm sized square-shaped Sn nanoparticles.[11] Yang et al. prepared C_4H_9-capped Sn nanoparticles by a reaction of $SnCl_4$ with Mg_2Sn in ethylene glycol dimethyl ether and subsequently with n-C_4H_9Li, but its XRD pattern clearly showed the large amount of SnO_2 contamination.[12] However, these studies were aimed at sensors. Recently, Wang et al. reported that amorphous Sn and Sn/SnO_2 core shell with particle sizes between 3 and 7 nm could be prepared from a phenanthroline and tin chloride complex; oxygen content was estimated to ∼10 wt % using X-ray photoelectron spectroscopy analysis.[13,14] However, initial specific capacity of the Sn nanoparticles was ∼600−700 mAh/g with irreversible capacity of ∼40−60%, and no cyclability data of it was provided.

Many materials such as Si, Al, Sn, Sb, and Bi are capable of accommodating Li and show Li storage capacities that are much higher than those of carbonaceous materials.[15] Graphite can store 372 mAh/g corresponding to LiC_6, and tin can store 970 mAh/g corresponding to $Li_{4.4}Sn$. However, those metals exhibited significant volume changes (>300%) that occur during Li alloying and dealloying, which causes cracking and crumbling of the electrode material and the consequent loss of electrical contact between the single particles, resulting in severe capacity loss.[16] Wolfenstine et al. suggested that a critical grain size of the fully lithiated $Li_{4.4}Sn$ particle at which microfracture would not occur would be ∼0.005 nm using a mechanical impact test method only but ignored initial particle size. In terms of electrochemical application, a critical particle size that induces catastrophic particle pulverization is much more important in a practical composite electrode.[17] Obtaining good capacity retention with alloy negative electrodes has proven to be difficult, except when the capacity is constrained to values close to graphite. The reason for failure is believed to be the inhomogeneous volume expansion in the coexistence regions of phases within different lithium concentrations with the same particles, resulting in particle pulverization.[18−23] This is particularly true for coarse-grained, macrostructured metals. However, mechanical strain can be reduced by tailoring the particle morphology of the Sn_xM_y (M = metals), particularly by

* Corresponding author. E-mail: jpcho@kumoh.ac.kr.
[†] Kumoh National Institute of Technology.
[‡] Pohang University of Science and Technology.
[§] Ulsan University.

(1) Schmid, G. *Nanoparticles*; Wiley-VCH: Weinheim, 2004. Rao, C. N. R.; Müller, A.; Cheetham, A. K. *Chemistry of Nanotechnologies*.
(2) Feldheim, D. L.; Foss, C. A., Jr. *Metal Nanoparticles*; Marcel Dekker: New York, 2002.
(3) Rotello, V. *Nanoparticles (Building Blocks for Nanotechnology)*; Kluwer Academic: New York, 2004.
(4) Bock, C.; Paquet, C.; Couillard, M.; Botton, G. A.; MacDougall, B. R. *J. Am. Chem. Soc.* **2004**, *126*, 8028.
(5) Lyon, J. L.; Fleming, D. A.; Stone, M. B.; Schiffer, P.; Williams, M. E. *Nano Lett.* **2004**, *4*, 719.
(6) Son, S. U.; Jang, Y.; Park, J.; Na, H. B.; Park, H. M.; Yun, H. J.; Lee, J.; Hyeon, T. *J. Am. Chem. Soc.* **2004**, *126*, 5026.
(7) Sun, S.; Murray, C. B.; Weller, D.; Folks, L.; Moser, A. *Science* **2000**, *287*, 1989.
(8) Bönnemann, H.; Brijoux, W.; Joussen, T. *Angew. Chem., Int. Ed.* **1990**, *29*, 273.
(9) Nayral, C.; Ould-Ely, T.; Maisonnat, A.; Chaudret, B.; Fau, P.; Lescouzeres, L.; Peyre-Lavigne, A. *Adv. Mater.* **1999**, *1*, 61.
(10) Schlecht, S.; Budde, M.; Kienle, L. *Inorg. Chem.* **2002**, *41*, 6001.
(11) Soulantica, K.; Maisonnat, A.; Fromen, M.-C.; Casanove, M.-J.; Chaudret, B. *Angew. Chem., Int. Ed.* **2003**, *42*, 1945.
(12) Yang, C.-S.; Liu, Y. Q.; Kauzlarich, S. M. *Chem. Mater.* **2000**, *12*, 983.
(13) Wang, Y.; Lee, J. Y.; Deivaraj, T. C. *J. Electrochem. Soc.* **2004**, *151*, A1804.
(14) Wang, Y.; Lee, J. Y.; Deivaraj, T. C. *J. Mater. Chem.* **2004**, *14*, 362.
(15) Wolfenstie, J.; Foster, D.; Read, J.; Behl, W. K.; Lueke, W. *J. Power Sources* **2000**, *87*, 1.
(16) Huggins, R. A. *Solid State Ionics* **1998**, *113*, 57.
(17) Courteny, I. A.; Dahn, J. R. *J. Electrochem. Soc.* **1997**, *144*, 2045.
(18) Graetz, J.; Ahn, C. C.; Razami, R.; Fultz, B. *Electrochem. Solid State Lett.* **2003**, *6*, A194.
(19) Wachtler, M.; Besenhard, J. O.; Winter, M. *J. Power Sources* **2001**, *94*, 189.
(20) Yang, J.; Wang, B. F.; Kang, K.; Liu, Y.; Xie, J. Y.; Wen, Z. S.; *Electrochem. Solid State Lett.* **2003**, *6*, A151.
(21) Kim, I.-S.; Blomgren, G. E.; Kumta, P. N. *Electrochem. Solid State Lett.* **2004**, *7*, A44.
(22) Lee, K. T.; Jung, Y. S.; Oh, S. M. *J. Am. Chem. Soc.* **2003**, *125*, 5652.
(23) Dong, Q. F.; Wu, C. Z.; Jin, M. G.; Huang, Z. C.; Zheng, M. S.; You, J. K.; Lin, Z. G. *Solid State Ionics* **2004**, *167*, 49.

10.1021/cm0504337 CCC: $30.25
Published on Web 06/04/2005

employing smaller particle sizes.[24−27] Despite these extensive efforts, Sn and tin alloys have not yet reached the reversible capacity of 900 mAh/g nor good capacity retention at higher C rates. Yang et al. reported that $Sn_{0.88}Sb_{0.12}$ particles smaller than 300 nm showed reversible capacity of 360 mAh/g even after 50 cycles, but did not show any evidence for particle size distribution and Sn phase formation.[28] However, $Sn_{0.88}Sb_{0.12}$ with a similar particle size to that reported above showed an initial capacity of 670 mAh/g, but capacity drastically decreased to 20 mAh/g after ∼30 cycles.[24] On the other hand, nanostructured SnO_2 nanofibers prepared from the template-synthesis method showed excellent capacity retention without losses after 800 cycles between 0.2 and 0.9 V.[29]

This paper reports for the first time the preparation of the size-controlled monomer-capped amorphous and crystalline tin nanoparticles using new capping agents: 2,4,6-tri(2-pyridyl)-1,3,5-triazine and 3-(2-pyridyl)-5,6-diphenyl-1,2,4-triazine. The results showed retained reversible capacity of >900 mAh/g and excellent cycling stability at higher C rates.

For preparing 2,4,6-tri(2-pyridyl)-1,3,5-triazine (**TT**) or 3-(2-pyridyl)-5,6-diphenyl-1,2,4-triazine (**DT**)-stabilzed tin metal particles, 0.7 mmol of tetraoctylammonium bromide as a catalyst was added to $SnCl_4 \cdot 5H_2O$ (0.9 mmol) in a solution of 15 mL of CH_2Cl_2 and deionized, deoxygenized water with vigorous stirring. A solution of DT or TT with 2.4 or 4.8 mmol in 100 mL of CH_2Cl_2 was added, and the resulting solution was stirred at room temperature for 20 min. $NaBH_4$ as a reducing agent (18 mmol) in 20 mL of deionized water was then added. The mixture was stirred for 1 h at room temperature under an argon atmosphere. After the reaction, the mixture was washed four times with water and acetone and evaporated in vacuo to yield the tin particles.The electrochemical studies were carried out using coin-type half cells (2106R type) with a Li counter electrode. The Sn nanoparticle:binder:carbon black in a weight ratio of 8:1:1 was used as the working electrode. The working electrode was made from the active material, Super P carbon black (MMM, Belgium), and polyvinylidene fluoride (PVdF) binder (Kureha, Japan). The electrodes were prepared by coating slurry onto a Cu foil followed by drying it at 110 °C for 20 min. The slurry was prepared by thoroughly mixing a *N*-methyl-2-pyrrolidone (NMP) solution of PVdF, carbon black, and the powdery active material. The coin-type battery test cells (size 2016) prepared in a helium-filled glove box contained a cathode, a Li metal anode, and a microporous polyethylene separator. The electrolyte was 1 M $LiPF_6$ with ethylene carbonate/diethylene carbonate/ethyl-methyl carbonate (EC/DEC/EMC) (30:30:40 vol %). We used standardized coin-cell parts (2016R-type), and normally the amount of the electrolyte was ∼0.1 g in each cell.[30,31] After cycling, tin particles were separated from the composite electrode by using ultrasonic rinsing in acetone and centrifugation.

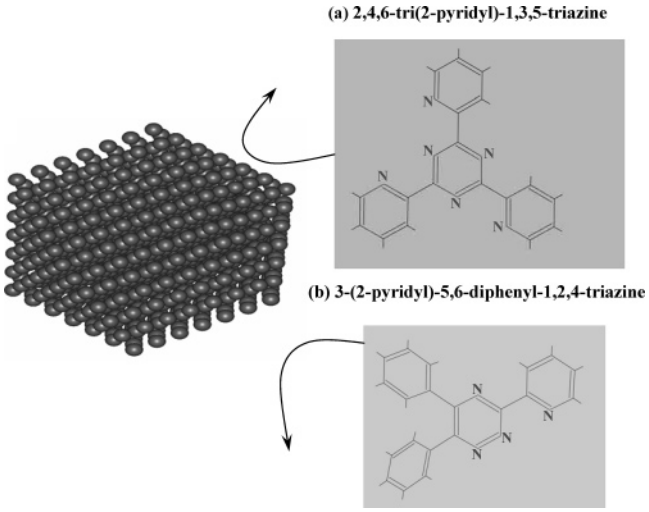

Figure 1. Structures of the monomers used for capping tin nanoparticles.

Figure 1 shows the chemical structures of the capping agents (monomers) used: 2,4,6-tri(2-pyridyl)-1,3,5-triazine (TT) and 3-(2-pyridyl)-5,6-diphenyl-1,2,4-triazine (DT). Figures 2a−d show the XRD patterns of the Sn nanoparticles synthesized using a capping monomer concentration of 2.4 and 4.8 mmol with TT (a, b) and with DT (c, d). All the diffraction peaks were indexed to tetragonal Sn (JCPDS #04-0673), and no impurity peaks are detected. The crystallite size of tin capped with 4.8 and 2.4 mmol of DT using the Scherrer formula was estimated to be 10 ± 0.5 nm and 20 ± 0.5 nm, respectively. The estimated particle size of the tin capped with 4.8 and 2.4 mmol of TT was 200 ± 5 nm and 300 ± 5 nm, respectively.

Figures 3a and b show TEM images of the tin nanoparticles prepared using 2.4 and 4.8 mmol of TT. Figures 3c and d show the TEM images of tin nanoparticles prepared using 2.4 and 4.8 mmol of DT. Further, elected area diffraction patterns of the 10- and 20-nm-sized Sn nanoparticles showed clear ring patterns, confirming formation of polycrystalline Sn phase (insets in Figure 3). The particle sizes appear to agree with those estimated from the XRD results. These results indicated that the resulting shapes can be changed by controlling the concentration of capping monomer. Compared to the Sn particles prepared using DT, which had all faceted shapes, those prepared using TT had a much lower particle size and its shape was more spherical. It is interesting to note the partial presence of a cubic shape in the 3-(2-pyridyl)-5,6-diphenyl-1,2,4-triazine (DT)-capped Sn. A cubic shape was reported to be generally obtained in the presence of weakly binding capping molecules.[32] Therefore, it is expected that TT binds much more strongly to the Sn surfaces than DT.

(24) Yang, J.; Takeda, Y.; Li, Q. Imanishi, N.; Yamamoto, O. *J. Power Sources* **2000**, *90*, 64.
(25) Yin, J.; Wada, M.; Yoshida, S.; Ishihara, K.; Tanse, S.; Sakai, T. *J. Electrochem. Soc.* **2003**, *150*, A1129.
(26) Yin, J.; Wada, M.; Tanase, S.; Sakai, T. *J. Electrochem. Soc*. **2004**, *151*, A583.
(27) Li, H.; Wang, Q.; Shi, L.; Chen, L.; Haung, X. *Chem. Mater*. **2002**, *14*, 103.
(28) Yang, J.; Wachtler, M.; Winter, Besenhard, J. O. *Electrochem. Solid State Lett.* **1999**, *2*, 161.
(29) Li, N.; Martin, C. R.; Scrosati, B. *Electrochem. Solid State Lett.* **2000**, *3*, 316.
(30) Cho, J.; Kim, Y. J.; Kim, T.-J.; Park, B. *Angew. Chem., Int. Ed.* **2001**, *40*, 3367.
(31) Cho, J.; Kim, Y.-W.; Kim, B.; Lee, J.-G.; Park, B. *Angew. Chem., Int. Ed.* **2003**, *42*, 1618.
(32) Lee, S.-M.; Jun, Y.; Cho, S.-N.; Cheon, J. *J. Am. Chem. Soc.* **2002**, *124*, 11244.

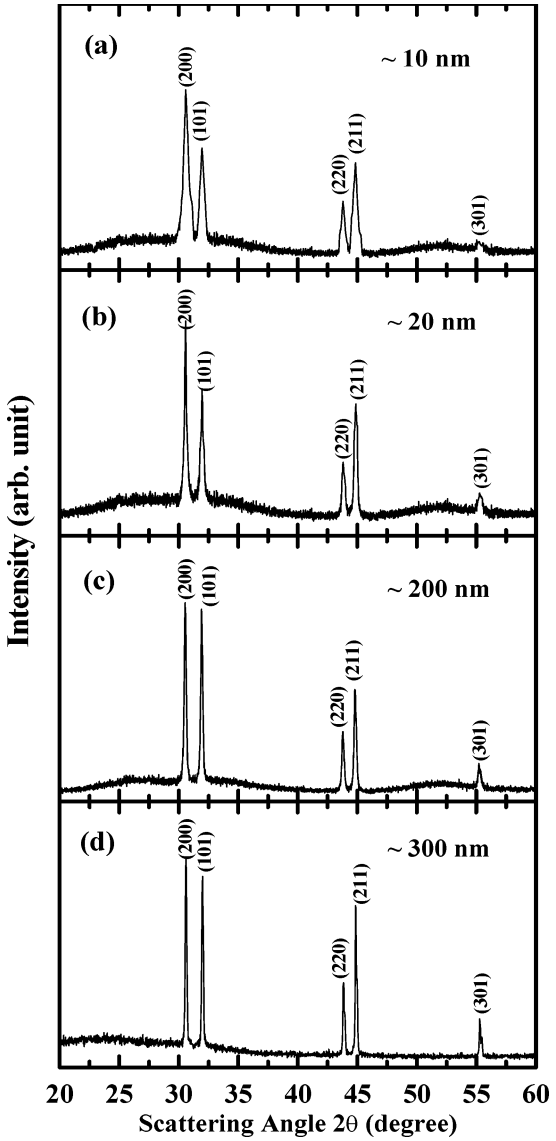

Figure 2. XRD patterns of the same tin particles used for the TEM observations in Figure 3. The ideal peak positions and intensities for the tetragonal Sn are marked (JCPDS #04-0673).

The reflective FT-IR spectra of the TT- and DT-capped Sn with particle sizes of 10 and 20 nm, respectively (see the Supporting Information) show that vibration bands of the capping agents appear to superimpose with capped Sn nanoparticles between 1200 and 650 cm^{-1}, indicating the presence of the capping agent on the particles. However, two intense bands of SnO_2 nanoparticle at 690 and 665 cm^{-1} can be distinguished from the others, and as-prepared capped Sn nanoparticles showed very small SnO_2 peaks. In general, SnO_2-contaminated Sn nanoparticles showed intensive broad peaks at ~27° and ~53° in the XRD patterns.[33] Although 2,4,6-tri(2-pyridyl)-1,3,5-triazine capping agent led to rather loosely aggregated Sn particles relative to a phenanthroline capping agent, it is very effective for both blocking reaction with oxyen and improving electrochemical properties. On the other hand, phenanthroline-capped Sn nanometals showed large irreversible capacity and low capacity retention.[13] Oxygen content was below 0.1 wt % from EDX analysis. To confirm the chemical state of TT- and DT-capped Sn nanoparticles with particle sizes of 10 and 20 nm, respectively, Sn L_{III}-edge XAFS characterization has been carried out on the BL7C (Electrochemistry) beamline at the Pohang Light Source (PLS), as shown in Figure 4. Sn L_{III}-edge XANES spectra (Figure 4a) of TT- and DT-capped Sn nanoparticles present peak feature similar to that of Sn metallic powder, directly meaning overall metallic state. It is also found out that the Sn metallic nanoparticles have been transformed to SnO_2-like phase by air oxidation. The existence of metallic Sn can be supported with EXAFS results. Figure 4b shows Fourier transform magnitudes of Sn L-edge EXAFS for TT- and DT-capped Sn nanoparticles, in comparison with those of reference Sn, SnO, and SnO_2 materials. SnO and SnO_2 oxides show typical FT peaks of Sn−O bonding at 1.63 Å for Sn^{4+}−O and 1.80 Å for Sn^{2+}−O (peak *A*) and Sn−O−Sn bonding above 3 Å (peak C), while Sn metal gives a FT peak of Sn−Sn metallic bonding at about 2.9 Å (peak *B*). For the TT- and DT-capped Sn, there are FT peaks of Sn−Sn metallic bonding at about 2.7 Å and Sn−C bonding in the surface region at 1.58 Å. The peak feature without the peak *C* means no noticeable surface oxidation of Sn since the peak C is associated with extended −[Sn−O−Sn]− bonding. As a result, the as-prepared Sn metallic state can be supported by help of the capping agent.

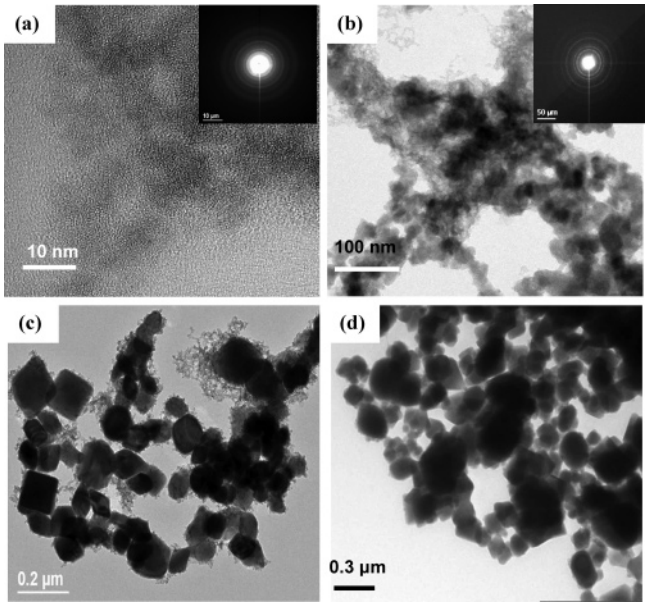

Figure 3. TEM images of the Sn nanoparticles capped with (a) and (b) 4.8 and 2.4 mmol of 2,4,6-tri(2-pyridyl)-1,3,5-triazine, respectively, and (c) and (d) 4.8 and 2.4 mmol of 3-(2-pyridyl)-5,6-diphenyl-1,2,4-triazine, respectively.

Figure 5 shows a comparison of the voltage profiles of the tin nanoparticles prepared using 4.8 and 2.4 mmol of TT (a,b) and DT (c,d) between 0 and 1.2 V at rates of 0.1 and 0.5 C for the first cycle and the remaining cycles, respectively. Overall, capacity retention was improved by decreasing the particle size. These results are similar to that reported by Yang et al.[28] However, Yang's work was limited by the particle size, which was >300 nm. Sn particles were also prepared using an identical method to Yang et al. using sodium citrate as the capping agent but this did not lead to

(33) Yang, C.-S.; Liu, Y. Q.; Kauzlarich, S. M. *Chem. Mater*. **2000**, *12*, 983.

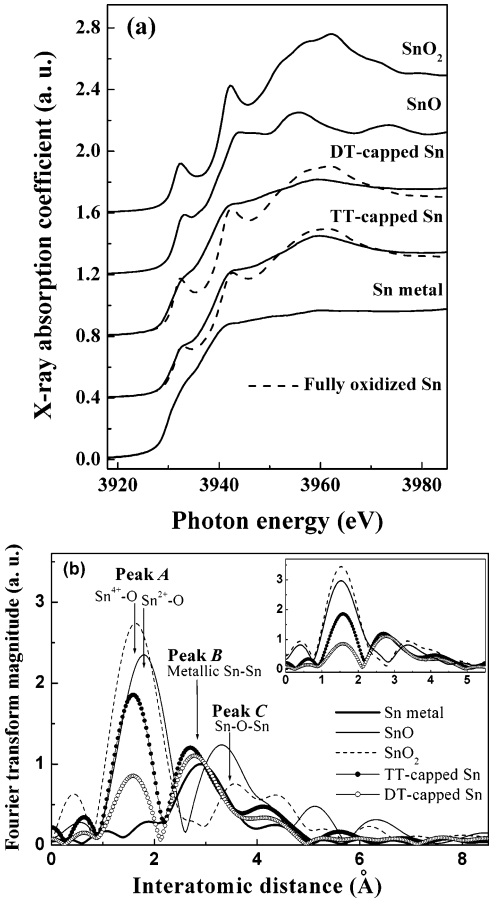

Figure 4. (a) Normalized Sn L_{III}-edge XANES features for 2,4,6-tri(2-pyridyl)-1,3,5-triazine (TT)- and 3-(2-pyridyl)-5,6-diphenyl-1,2,4-triazine (DT)-capped Sn nanoparticles, in comparison with those of Sn, SnO, and SnO_2 reference materials. Dashed lines mean their XANES spectra after full oxidation of the capped Sn particles. (b) Fourier-transformed (FT) magnitudes of Sn L_{III}-edge k^3-weighted EXAFS spectra. Inset figure presents FT peak feature variation after full oxidation for the TT (solid) and DT (dashed) capped Sn nanoparticles.

a controlled particle size. During the reduction of Sn^{4+} into Sn°, the Sn particles aggregated into micrometer-sized particles. On the other hand, sodium citrate was a very effective capping agent for controlling the particle size and 10-nm-sized Ag nanoparticles were easily prepared using this capping agent.[34,35] Even though previous studies showed that the surface area of a metal increases with decreasing particle size, the amount of Li that was irreversibly consumed during SEI (solid electrolyte interface) formation should also increase. Hence, the decreasing particle size results in an increased irreversible capacity. However, our results clearly showed that a smaller tin size retained good reversible capacity, and a ~10 nm-sized tin showed 87% reversible capacity. Moreover, ~10-nm and ~20 nm-sized Sn exhibited charge capacities of 1000 and 940 mAh/g, respectively, and the ratios of the irreversible capacities were 87% and 90%, respectively. On the other hand, the irreversible capacity was slightly reduced as the particle size increased and ~200- and ~ 300-nm-sized Sn showed 90% and 93%, respectively, but the charge capacities of these were decreased to 940 and 916 mAh/g, respectively. Origin of the irreversible capacity may be due to partial reaction of the capping agent with the electrolyte during first cycling.

(34) Jana, N. R.; Gearheart, L.; Murphy, C. J. *Chem. Commun*. **2001**, 617.
(35) Murphy, C. J.; Jana, N. R. *Adv. Mater*. **2002**, *14*, 80.

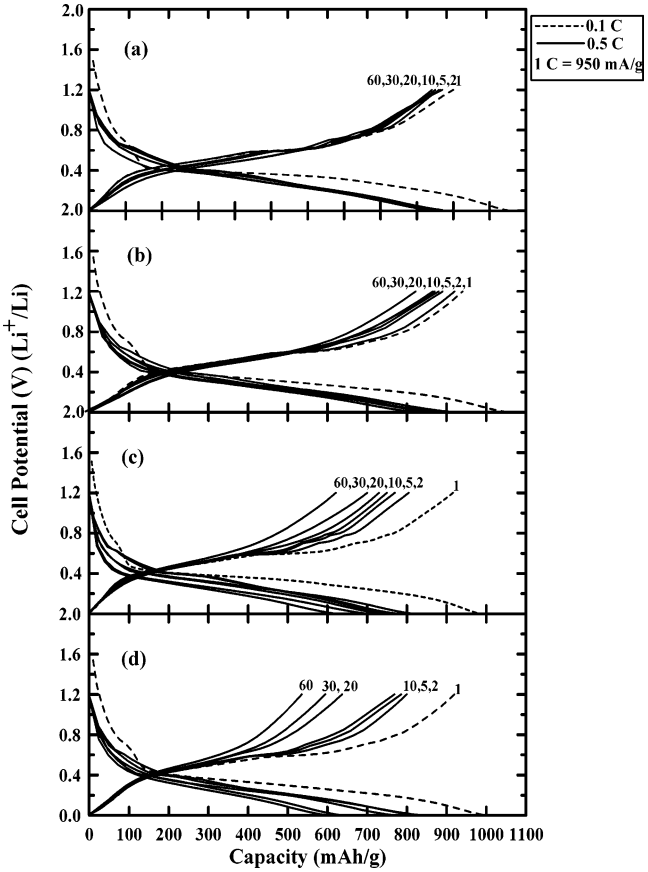

Figure 5. Voltage profiles of the Sn nanoparticles as a function of (a) ~10 nm, (b) ~20 nm, (c) ~200 nm, and (d) ~300 nm in coin-type half cells. The Sn anodes were cycled at the rate of 95 mA/g for the first cycle and at charge and discharge rates of 475 mA/g between 1.2 and 0 V for the remaining 29 cycles.

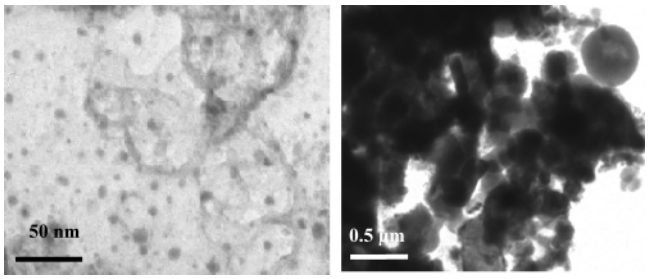

Figure 6. TEM images of the capped Sn nanoparticles with particle sizes of ~10 and ~300 nm after 60 cycles.

In addition, the capacity retention of the Sn nanoparticles decreased from 94%, 87%, 68%, and 58% at the 0.5 C rate after 60 cycles as the particle size increases from ~10, ~20, ~200, and ~300 nm, respectively. Figure 6 exhibits the TEM images of the Sn particles with particle sizes of ~10 and 300 nm capped with TT and DT, respectively, after 60 cycles. TT-capped Sn retained the original particle size distribution without aggregation as opposed to DT-capped Sn which showed severe particle aggregations and growth. This result indicates that DT strongly bonded on the particle surface acts as inhibitors for particle aggregation. In addition, we observed that TT-capped Sn electrodes of the after cycling showed good adhesion on the current collector while the DT-capped sample was severely separated from the current

collector. In consequence, TT-capped tin nanoparticles significantly reduce the formation of surface cracks induced from the volume change in the Li_xSn_y phase, and therefore diminishes the repetitive formation of electrode/electrolyte interfaces affecting the capacity fading.

In conclusion, monomer-capped Sn nanoparticles with a particle size of ~10 nm exhibited a much improved capacity and cycling stability than the Sn−C composite or Si−C composites[21−23] showing an initial capacity of ~1000 mAh/g and no capacity fading at the higher C rate. This performance is superior to the mesoporous carbon (ratio of the irreversible capacity was 64% and the initial charge capacity was 1147 mAh/g) and mesoporous tin phosphate/$Sn_2P_2O_7$ composite (ratio of the irreversible capacity was 25% and initial charge capacity was 720 mAh/g).[36,37] In terms of the irreversible capacity, the monomer-capped Sn was comparable to the commercially used graphite anode materials (~7−13%).

Acknowledgment. We are grateful to authorities of Pohang Light Source (PLS) for XAS measurements. The experiments at PLS were supported in part by Korea MOST and POSTECH. This work was supported by University IT Research Center Project, and by the Basic Research Program (R01-2004-000-10173-0) of KOSEF.

Supporting Information Available: Additional figure (PDF). This material is available free of charge via the Internet at http://pubs.acs.org.

CM0504337

(36) Zhou, H.; Zhu, S.; Hibino, M.; Honma, I.; Ichihara, M. *Adv. Mater.* **2003**, *15*, 2107.
(37) Kim, E.; Son, D.; Kim, T.-G.; Cho, J.; Park, B.; Ryu, K.; Chang, S.; *Angew Chem., Int. Ed.* **2004**, *43*, 5897.